Accepted Manuscript

Title: Process Parameters for Hot Stamping of AA7075 and D-7xxx to Achieve High Performance Aged Products

Authors: Kaab Omer, Atekeh Abolhasani, Samuel Kim, Tirdad Nikdejad, Clifford Butcher, Mary Wells, Shahrzad Esmaeili, Michael Worswick

PII: S0924-0136(18)30095-5
DOI: https://doi.org/10.1016/j.jmatprotec.2018.02.039
Reference: PROTEC 15666

To appear in: *Journal of Materials Processing Technology*

Received date: 29-4-2017
Revised date: 13-2-2018
Accepted date: 25-2-2018

Please cite this article as: Omer K, Abolhasani A, Kim S, Nikdejad T, Butcher C, Wells M, Esmaeili S, Worswick M, Process Parameters for Hot Stamping of AA7075 and D-7xxx to Achieve High Performance Aged Products, *Journal of Materials Processing Technology* (2010), https://doi.org/10.1016/j.jmatprotec.2018.02.039

Process Parameters for Hot Stamping of AA7075 and D-7xxx to Achieve High Performance Aged Products

Kaab Omer[1*], Atekeh Abolhasani[1], Samuel Kim[1], Tirdad Nikdejad[1], Clifford Butcher[1], Mary Wells[1], Shahrzad Esmaeili[1], Michael Worswick[1]

[*]Corresponding author:

komer@uwaterloo.ca

[1] University of Waterloo
200 University Ave W
Waterloo, Ontario, Canada
N2L 3G1

Abstract

This work examines the necessary process parameters for die quenching (DQ) during hot stamping and subsequent age hardening and paint bake cycle (PBC) response for two alloys: AA7075 and a developmental 7xxx alloy (referred to as AA7xxx), with a lower Chromium content, higher Zirconium content and higher Zinc-to-Magnesium ratio in comparison to AA7075. For both alloys, a minimum solutionizing time of 8 minutes was found to be required, along with a minimum quench rate of 56°C/s and 27°C/s for AA7075 and AA7xxx, respectively. Two-step aging treatments, leveraging a paint bake cycle (PBC) of 177°C for 30 minutes as the second step, were considered after die quenching and were devised to achieve T6- or T76-level strengths. For AA7075, an aging treatment of 120°C for 8 hours, followed by the paint bake cycle (PBC) produced strength levels similar to a T6 temper. DSC experiments showed that the

microstructure from this heat treatment was similar to a peak-aged T6 temper. For AA7xxx, a treatment of 100°C for 4 hours and followed by the paint bake produced a strength similar to a T76 temper, while 120°C for 3 hours followed by the paint bake yielded T6 strength levels. The properties of the custom aging treatments were validated through tensile tests. The resulting stress-strain curves show that it is possible to achieve T6 or T76 properties using a custom aging treatment incorporating the PBC that is 65-83% shorter than standard T6 or T76 treatments.

Keywords: Die Quenching, Paint Bake Cycle, Solutionizing, Quench Rate, High Strength, AA7075, AA7xxx

1. Introduction

The transportation industry is under increasing pressure to improve fuel economy and vehicle safety. In the field of sheet metal forming, significant weight reductions may be possible using precipitation-hardenable 7xxx-series aluminum alloys with specific ultimate tensile strengths that are comparable to that of high strength steels but with a density only one-third that of steel. 7xxx-series alloys are extensively used for aircraft; however, their processing costs need to be reduced for automotive applications. Additionally, the low room temperature formability of 7xxx series alloys severely limits the types of structural components that can be stamped, although there is some potential for warm forming at moderate temperatures such that the desired final temper is not significantly affected (Wang et al., 2012).

The hot stamping process, or die quenching (DQ) process, is considered a viable alternative to realize the benefits of the 7xxx series alloys in manufacturing high performance automotive parts. The DQ process involves the simultaneous forming and quenching of a solutionized

aluminum blank using a chilled die (Mohamed et al., 2012). The part is then removed from the die and subjected to additional thermal treatments (artificial aging) to control the precipitation hardening process and achieve the desired mechanical properties (Deschamps et al., 2012).

There are a number of uncertainties associated with the DQ process for 7xxx series aluminum alloys. Determining the minimum amount of time required to solutionize the alloys prior to die quenching is critical. At present, most investigations that involve the solutionizing of these alloys employ a soak time of at least 30 min. Examples of these investigations are reported by Erdoğan et al. (2014) for AA7075 and by Chen et al. (2012) for AA7085. However, from a metal forming perspective, a 30 min soak time is a severe limitation for its adoption into a production environment. A 10 minute soak time was employed by Atkinson et al. (2008) but unfortunately, there was no rationale provided for this duration by the authors.

The transfer time, which is the amount of time elapsed from the moment that the blank is removed from the oven to the moment that it makes contact with the dies, is also a critical factor in the DQ process. Liu et al. (2010) showed that the critical temperature (i.e., the temperature below which solute precipitation becomes significant) for AA7075-T6 was 415°C and 367°C for AA7085-T76 if cooling rates are slow. Yang et al. (2016) showed that the critical temperature of AA7150 decreases from 400°C when cooled at 3°C/s to 250°C when cooled at 300°C/s. A similar conclusion was reached by Zhang et al. (2016) for AA7020.

In a DQ metal forming operation, the quench rate is expected to increase with increasing contact pressure (Caron et al., 2014). The results of Liu et al. (2010) show that alloys such as AA7085 do not display as much quench rate sensitivity as AA7075. Insensitivity to quench rate means that AA7085 can be die quenched at lower forming pressures and still be sufficiently age hardenable

afterwards. In 7xxx series alloys, a lower quench rate leads to greater heterogenous solute precipitation and the loss of excess vacancies (Fabian and Wolter, 1991). A lower quench rate also leads to lower solute concentration when the quenched material reached room temperature (Starink et al., 2015), and therefore, a loss of strength from the smaller volume fraction of hardening precipitates available (Zhang et al., 2014). Collectively, these factors hinder precipitation hardening and make the quenched material less age hardenable than it would be under a higher quench rate. Deformation at elevated temperatures has been found to promote the formation of precipitates (Rajamuthamilselvan and Ramanathan, 2011) that limit the age hardening potential of the as-quenched material.

After the die quenching operation is complete, the next step for the formed part is the artificial aging treatment to bring the dissolved precipitates out of the supersaturated solid solution (SSSS) to harden the material. The temperature and duration of the aging process are important to control the mechanical properties of the part and can also impact corrosion resistance (Clark et al., 2005). From an applicability perspective, particularly in the automotive sector, most formed parts, including those that comprise a part of the body structure, will also have to undergo a paint bake cycle (PBC) at a temperature of 177-185°C for approximately 20-40 minutes. Sevim et al. (2014) have shown that peak aging conditions occur after 4 hours at 185°C on supersaturated AA7075. Jabra et al. (2006) have shown that T6 tempered AA7075 begins to overage after being exposed to 180°C for just 15 minutes. These findings raise the question of what effect the PBC may have on the properties of 7xxx-series aluminum components with various thermomechanical processing histories.

The objectives of the present work are (a) to investigate the aforementioned challenges with the DQ process for AA7075 and a developmental 7xxx alloy (henceforth referred to as AA7xxx),

with a lower Chromium content, higher Zirconium content and higher Zinc-to-Magnesium ratio (see Section 2) in comparison to AA7075, and (b) to develop a thermal processing route to impart mechanical properties that are desired for an automotive structural component for crash applications. To achieve these objectives, parametric studies were performed to identify the process parameters such as transfer time (from oven to die), solutionizing time and minimum required quench rates for the material to enter an SSSS after forming. In addition, the influence of the artificial aging process parameters and PBC were also explored via hardness measurements and tensile testing at quasi-static strain rates (0.001 s^{-1}).

2. Experimental Procedure

The mechanical behaviour of the AA7075 and AA7xxx alloys resulting from implementing various thermal processing routes were evaluated using both tensile experiments and Vickers hardness measurements. Both alloy sheets were 2.0 mm in thickness. Measured chemical compositions for AA7075 and nominal compositions for the developmental AA7xxx alloy are reported in Table 1. The chemical composition for AA7075 was measured using inductively coupled plasma, while the AA7xxx values were supplied with the material by Arconic Ground Transportation Group. The key differences between the commercial AA7075 and the developmental AA7xxx alloy are that AA7xxx has a lower Chromium content and a higher Zirconium content; both are known to reduce quench sensitivity. The Zinc-to-Magnesium ratio was also higher in the AA7xxx in comparison to AA7075.

Table 1. Chemical composition for AA7075 (measured) and for the developmental AA7xxx alloy (nominal).

Elements	AA7075	AA7xxx
Aluminum	90.07%	87.6-90.4%

Zinc	6.35	7.0-8.0
Magnesium	1.92	1.2-1.8
Copper	1.46	1.3-2.0
Zirconium	Negligible	0.08-0.15
Iron	0.10	0.08
Chromium	0.10	0.04

All of the uniaxial tensile experiments were conducted using a standard ASTM-E8 ("Standard Test Methods for Tension Testing of Metallic Materials," 2015) geometry at a quasi-static strain rate of $0.001s^{-1}$. At least three repeat tests were performed for each of the process conditions in this work. Unless otherwise specified, the tensile tests were conducted on samples cut along the rolling direction. Full field strain measurements were obtained using a commercial stereoscopic digital imaging correlation (DIC) software, Vic-7 (Correlated Solutions, 2013), using a 50 mm virtual extensometer for evaluation of the mechanical properties. The DIC setup consisted of two Point Grey GRAS-50S5M-C cameras mounted onto a tripod. A set of Nikon AF Micro 60 mm lenses were attached to the Point Grey cameras. The DIC analysis employed a step size of 2 and a strain filter of 5 pixels.

Three Vickers micro-hardness measurements were performed through the thickness of the sheet (on the surface defined by the rolling direction of the sheet), using a LECO MHT Series 2000 hardness tester and 1kg indenter load. The through-thickness sheet samples were mounted in a resin/hardener mixture and polished using SiC sandpaper with a grit size of 2400. All of the hardness values presented herein are the average of the through-thickness hardness measurements.

The quenching experiments were performed in a hydraulic press between two flat dies, shown in Figure 1. AA7075 and AA7xxx blanks measuring 75 mm x 75 mm were solutionized in a convection oven at 470°C (The Aluminum Association, 2009). Three repeat experiments were conducted for each experimental condition. The blanks contained a 19 mm diameter cutout at the centre (shown in Figure 2). A K-type thermocouple was attached, using thermal tape, to the edge of the cutout to record the temperature-time history of the blank (also shown in Figure 2). After soaking at 470°C, the blank was transferred from the oven to the press, where it was quenched at a given rate.

Figure 1. Flat dies used to quench the aluminum blanks. Details of the die geometry can be found in Caron et al. (2014). The dies were made out of tool steel.

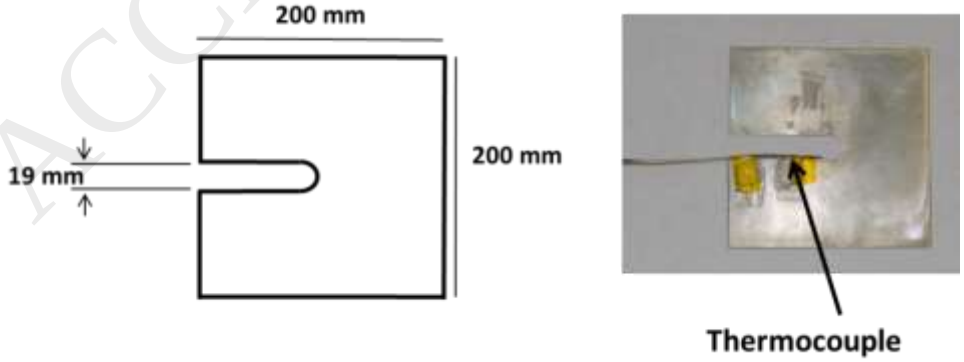

Figure 2. Thermocouple attached into the cutout of the 75 mm x 75 mm blank.

The quench rate was controlled using press tonnage, which controlled the contact pressure between the dies and the blank. Since the quench rate was not linear with respect to time, a fitting scheme was used to identify a representative quench rate. All representative quench rates in this work were determined by fitting a straight line onto the temperature-time curve of the blank in the range of 400-70°C (as shown in Figure 3). The fit was performed using a linear least squares regression, with R^2 values ranging from 0.82 to 0.91. The slope of the resulting line was assumed to be the representative quench rate at the given pressure. Table 2 shows the die pressures used in this work and their equivalent quench rates.

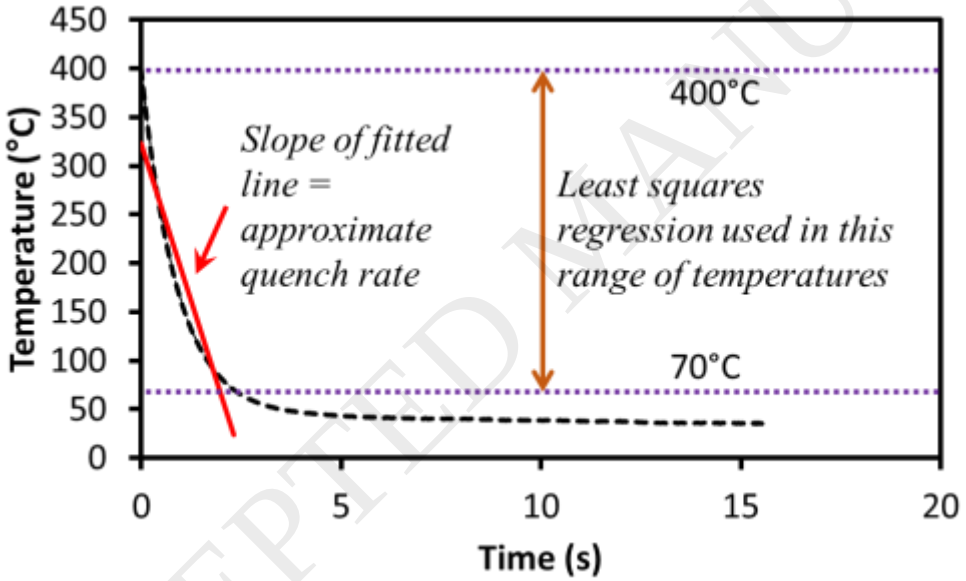

Figure 3. Example showing the identification of the equivalent quench rate of 56°C/s in the range from 400-70°C for an AA7075 sample at a die pressure of 40 MPa and transfer time of 6s.

Table 2. Die pressures and corresponding quench rates obtained using the least squares method in Figure 3

Die Contact Pressure (MPa)	Equivalent Quench Rate (°C/s)
5	27
12.5	34
25	40
40	56

60	128

3. Mechanical Properties of the As-Received Materials

The two alloys investigated in this work were commercially produced AA7075-T6 and AA7xxx-T76. The T6 designation indicates the AA7075 has been aged to "peak strength" and the T76 temper of the AA7xxx denotes the material has been slightly overaged from the peak T6 condition. The mechanical properties from tensile experiments for both alloys in their as-received tempers are provided in Table 3. Stress-strain curves in the rolling and transverse directions are shown in Figure 4. Neither of the two alloys shows significant anisotropy in the stress response, however, the R-values (*i.e.*, the ratio of the plastic width strain to the through-thickness plastic strain) varied significantly with material direction (Table 3).

Table 3. Measured mechanical properties (*i.e.*, properties derived from the stress-strain curves such as Young's modulus, yield stress and ultimate tensile stress), R-values and stress ratios (the ratio obtained when dividing the stress obtained from tensile testing in one direction by the stress obtained from testing in another direction) for AA7075-T6 and AA7xxx-T76

Alloy and Temper Property	AA7075-T6	AA7xxx-T76
Young's Modulus (GPa)	69	69
Yield Strength (MPa)	483	486
Ultimate Tensile Strength (MPa)	566	556
Vickers Hardness (HV)	180	168
R_0	0.7	0.5
R_{45}	0.9	1.2
R_{90}	1.0	1.9
Stress Ratio (Transverse-to-Rolling)	1.003	1.002
Stress Ratio (Diagonal-to-Rolling)	0.984	0.987
Elongation at fracture	0.15	0.13 (Rolling); 0.15 (Transverse)

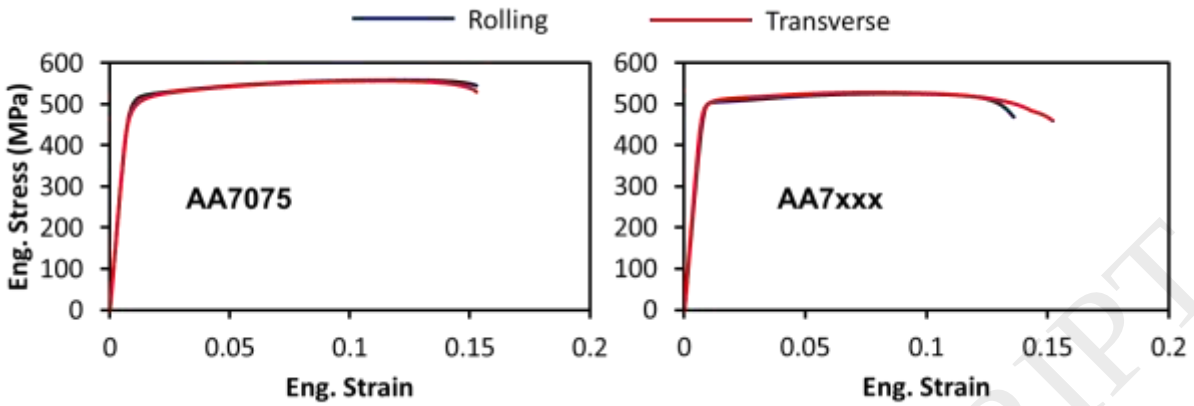

Figure 4. Measured stress-strain curves for as-received AA7075-T6 and AA7xxx-T76.

4. DQ Process Parameters

The DQ process parameters investigated were: solutionizing time, transfer time, quench rate and artificial aging treatments. Each of the following subsections will discuss one of the aforementioned parameters in the order they were stated. A brief literature review is provided for each parameter, followed by the experimental methodology employed and results. It is noted that a solutionizing temperature of 470°C was selected based on recommendations found in The Aluminum Association (2009).

4.1. Solutionizing Time

4.1.1. Experimental Setup

The objective of the experiments reported in this section was to determine the minimum time required to solutionize these two alloys in a standard convection oven. The solutionizing time experiments in this work were conducted as follows:

- Blanks were placed in a convection oven for 2.5 min, 5 min, 8 min, 15 min and 30 min. An example temperature-time profile for AA7xxx is shown in Figure 6.
- The blanks were quenched using a rate of 56 °C/s

- Microhardness measurements were taken 24 h and 3 weeks after the quench on the same samples, in order to ascertain the amount of natural aging that had taken place

4.1.2. Results

Figure 5 shows Vickers hardness measurements that were conducted on the quenched and naturally aged AA7075 and AA7xxx samples. The points in the plot represent average Vickers hardness based on the nine measurements conducted (three through-thickness measurements on each of the three repeated samples). Error bars depicting standard deviation are also shown. For reference, the hardness of the as-received material is also shown.

The hardness data acquired 15 min after quenching shows that the measured hardness decreases with respect to solutionizing time, up to 8 minutes. After a solutionizing time of 8 minutes, the hardness remains steady at 68 HV for AA7075 and 72 HV for AA7xxx. Hardness measurements conducted 24 hours after quenching reveal a constant hardness value of 130 HV for AA7075 and 136 HV for AA7xxx, for all soak times. The hardness three weeks after quenching shows greater natural aging for soak times of 8 minutes or more. The lower natural aging response for specimens soaked for five minutes or less indicates that neither alloy was properly solutionized for such low soak times. For the soak times of eight minutes or more, the AA7075 experienced an average hardness increase of 85 HV in three weeks and the AA7xxx experienced an average increase of 69 HV. This average increase in hardness remained fairly constant for soak times longer than 8 minutes, suggesting that there is no obvious benefit accrued through longer solutionizing times.

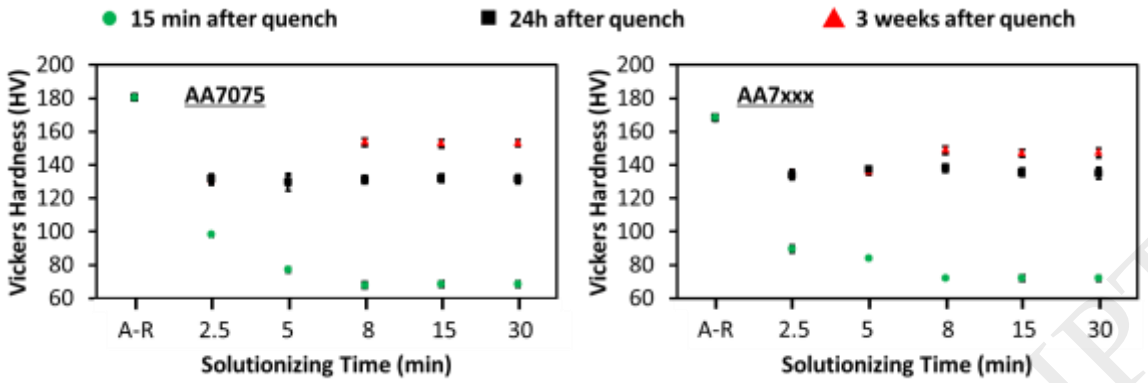

Figure 5. Hardness measurements as a function of solutionizing time, 15 min (green), 24h (black) and 3 weeks (red) after quenching. A-R represents the hardness of the as-received material.

The requirement for an 8-minute soak time in order to solutionize the blank is also supported by the measured thermal histories shown in Figure 6 for an AA7075 sample (the temperature-time profile of the AA7xxx sample was almost identical to the AA7075 sample). As shown in the figure, it took the sample approximately 6.5 minutes to reach the desired solutionization temperature of 470°C. As such, a *total* time of 8 min corresponds to 90s at 470°C.

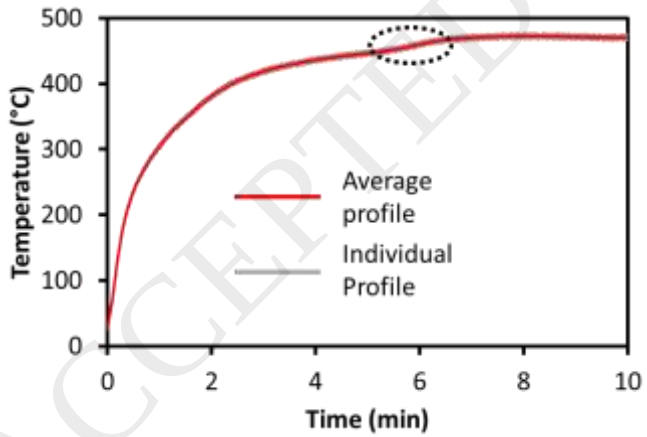

Figure 6. Temperature-time profile in the AA7xxx blank as it heats up in a free convection oven.

The temperature time-profile in Figure 6 also displays a consistent inflection point at approximately 5.5 minutes that is followed by a resumption of the temperature increase. This delay in the continuous temperature profile is thought to be associated with final dissolution of

the precipitates present in the as-received sheet alloys. Such time history behavior has also been observed by Xie et al. (2003) for AA7050 and by Zhang et al. (2007) for AA7075. Similarly, calorimetric studies on AA7075-T6 by Viana et al. (1999) showed an endothermic peak at 440°C, which is consistent with the inflection point observed at the same temperature in Figure 6.

4.2. Effect of Transfer Time

4.2.1. Experimental Setup

Two transfer times were investigated: 6s and 15s; these were selected as being representative of a relatively short *versus* a relatively long time to remove a blank from a furnace and then position within a tool in an automated industrial process. To quantify the transfer time effect, tensile specimens were solutionized and quenched at a rate of 56°C/s and tested immediately (i.e., 7-8 minutes after quenching) and after six days of natural aging.

4.2.2. Results

Figure 7 shows the engineering stress-strain curves obtained from the tensile tests. As evidenced by the stress-strain curves, the longer transfer time did not have a strong effect on the hardening response for either alloy. For both alloys, there was a significant increase in strength after a natural aging period of six days had elapsed. The AA7075 was shown to lose some elongation when a transfer time of 15s was used, whereas this was not observed in the AA7xxx.

The drop in temperature during transfer between the furnace and press is shown in Figure 8 for AA7075. Referring to Figure 8, the temperature-time profile shows that after 6s, the temperature was approximately 412°C and after 15s, the temperature was 360°C. The temperature-time profiles for AA7xxx were found to be almost identical to those for AA7075. The results plotted

in Figure 7 and Figure 8 show that AA7075 drops well below its critical temperature of 412°C (Liu et al., 2010) after a 15s transfer time. Noting the fact that the cooling rate during the transfer stage is slow (*i.e.*, on the order of 1°C/s), it is very likely that precipitation began in AA7075 during the 15s transfer. Based on the results of Yang et al. (2016) for AA7150 and Zhang et al. (2014) for AA7020, the likely precipitates formed during this time are Al_2MgCu and $Mg(Al,Cu,Zn)_2$. The formation of these precipitates can explain the loss of ductility experienced by AA7075 during the 15s transfer.

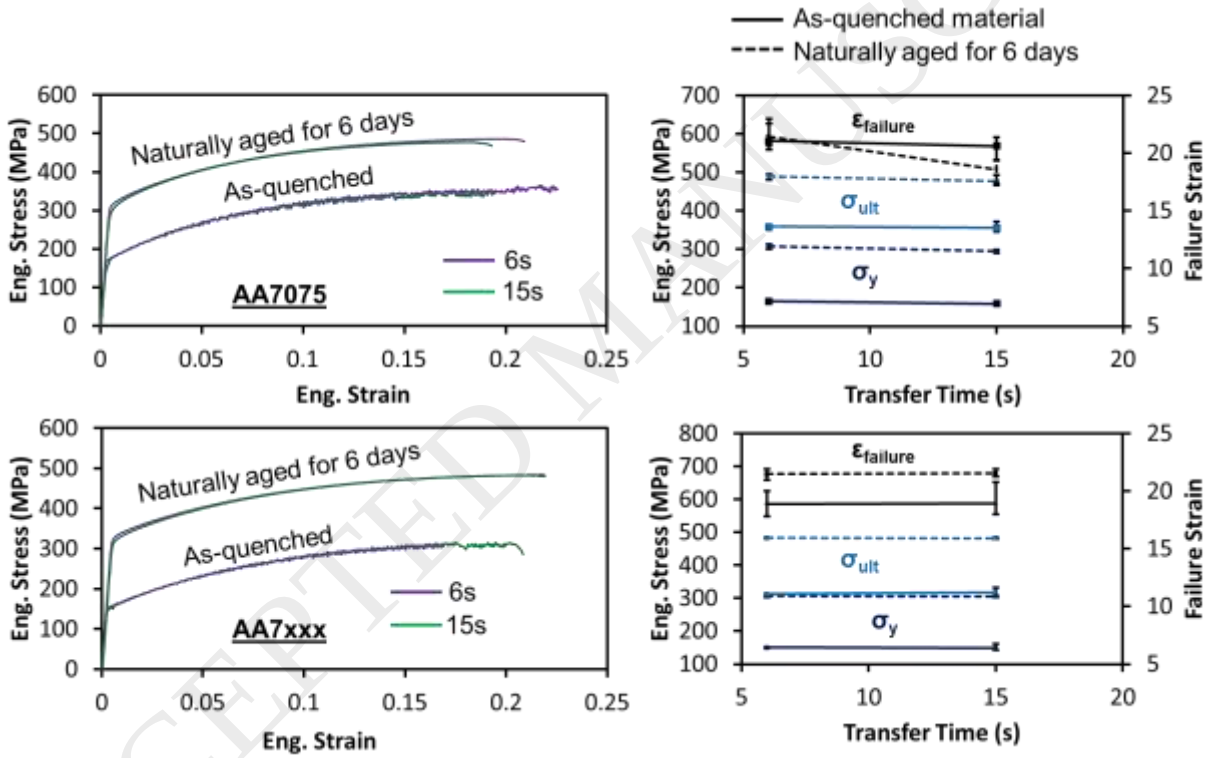

Figure 7. Engineering stress-strain curves for different transfer times. The material was solutionized, quenched at 56°C/s and then tensile tested.

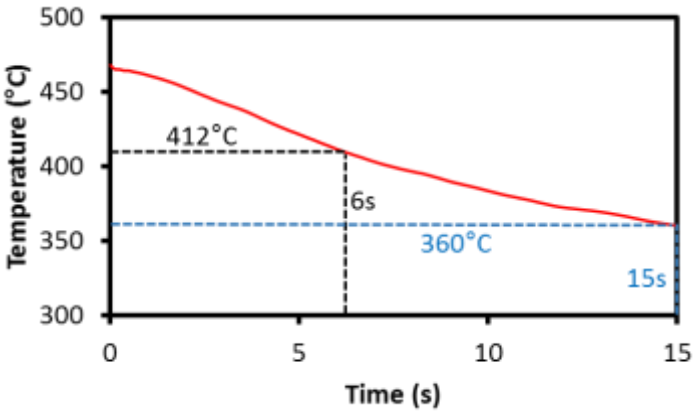

Figure 8. Temperature-time profile of a solutionized AA7075 tensile specimen as it cools in room temperature air during a 15s transfer from oven to die.

4.3. Effect of Quench Rate

4.3.1. Experimental Setup

To investigate the effect of quench rate, samples were heated for 8 min and quenched at the quench rates shown in Table 2, following a transfer time of 6s. Micro-hardness measurements were conducted 15 min, 24h and three weeks after the quenching process, in order to determine the extent of natural aging between these times. Tensile tests were also conducted, immediately after (i.e., within 8 minutes) the quenching process and after six days of natural aging, on samples quenched at the following approximate cooling rates: 25°C/s, 40°C/s and 60°C/s.

4.3.2. Results

Micro-hardness measurements of the die quenched alloys kept at room temperature after quenching as a function of quench rate (along with the corresponding quench pressures) are presented in Figure 9. The micro-hardness measurement results indicate that the AA7075 natural age hardening response is strongly dependent on quench rate. The AA7075 specimens quenched at rates of 40°C/s and higher and all of the AA7xxx samples exhibited a hardness of 150 and 146 HV, respectively, after quenching and three weeks natural aging. The lower quench rate AA7075

samples (27 and 34°C/s) exhibited somewhat higher hardness levels after quenching. While all of the samples displayed a similar response to natural aging after 24 h, the lower quench rate AA7075 samples attained a lower hardness level after two weeks.

To further examine the effect of quench rate on aging, Figure 10 shows the temperature-time profiles of the AA7075 samples quenched at the five rates in Figure 9. Of interest is the duration of time at which the material resides within its critical temperature range (the temperature range over which precipitation is significant) which, for AA7075, is 185-412°C. The AA7075 samples resided in the critical temperature range for 3.9s and 4.7s for the quench rates of 27 and 34°C/s, respectively, as opposed to 0.8, 2.5 and 3.2s for the higher rates. The longer durations for which the lower quench rate AA7075 samples spent in the critical temperature range likely resulted in precipitation during quenching and accounts for the lower initial as-quenched hardness levels.

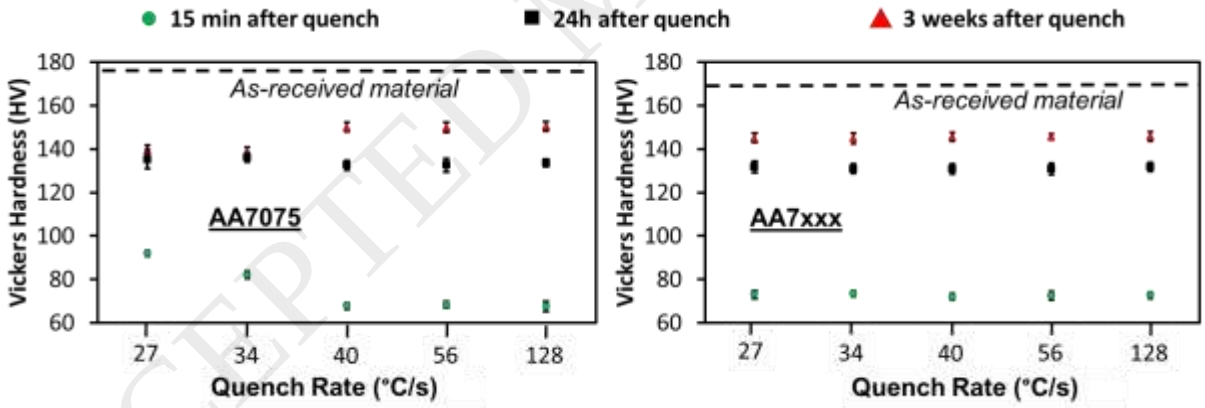

Figure 9. Hardness measurements of quenched materials at different cooling rates.

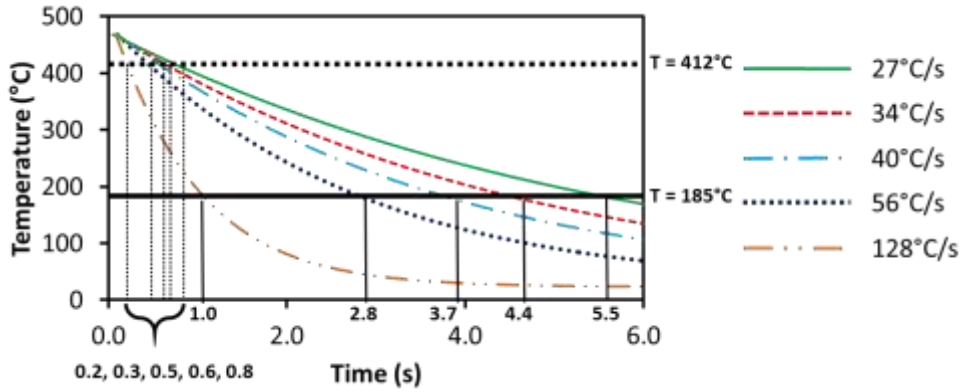

Figure 10. Temperature-time profiles of AA7075 quenched at the five rates in Figure 9. The times at which the material cooled below its critical temperature range (i.e., below 412 and 185°C) are indicated on the x-axis for each of the five quench rates. The dashed black lines indicate time taken to cool to 412°C. The black lines indicate time to 185/187°C.

The solute depletion during quenching at the lower rates would also account for the lower natural aging response. These results are consistent with the reports of Liu et al. (2010) on another quench-sensitive 7000-series alloy, AA7055, which experiences a 20% greater solute depletion when quenched at 20°C/s as opposed to 30°C/s (Starink et al., 2015). For AA7075, the lower quench rate may also promote the formation of Mg_2Si (Zhang et al., 2014) and $Mg(Zn,Cu,Al)_2$ precipitates (Yang et al., 2016) during cooling. The formation of such precipitates reduced the supersaturation level of the alloy once it reaches room temperature, and therefore, reduces its age hardenability. For quench rates in the range of 40-128°C/s, the AA7075 hardened by approximately 87 HV over a two-week period. The AA7075 hardness data exhibited a plateau, implying that the increase in the quench rate beyond 40°C/s does not provide additional hardening due to natural aging.

The developmental AA7xxx alloy did not exhibit sensitivity to quench rate for the range of quench rates considered, since the alloy hardness measured 15 minutes after quenching was independent of the quench rate and it naturally aged by the same amount for each quench rate. The critical temperature range has not been established for this alloy; however, its lower quench

sensitivity can be explained by comparing its compositional range to those of other alloys known to exhibit low quench sensitivity (Table 4). In general, it has been well established that both Cr and Zr affect recrsytallization, as well as quench sensitivity (Conserva et al., 1971). Liu et al. (2007) found that a low chromium content in 7000-series alloys promotes lower quench sensitivity. Based on the finding of Liu et al. (2007), the chromium present in AA7075 results in large incoherent dispersoids which act as nucleation sites for heterogenous precipitation. During a rapid quench, there is not enough time for precipitates to form around the dispersoids and thus the material will have a high level of supersaturation, which will promote greater age hardening. However, during a slow quench, there will be enough time for precipitation to occur at high temperatures at these nucleation sites, resulting in lower excess solute availability for further age hardening.

Table 4. Nominal fractions by mass (ASM International, 1990) of Zirconium and Chromium for high quench sensitivity AA7075 versus those of AA7010, AA7050, and AA7085 which exhibit low quench sensitivity. Also indicated are the levels for the current developmental AA7xxx alloy.

Elements	**AA7075**	**AA7xxx**	**AA7010**	**AA7050**	**AA7085**
Zirconium	Negligible	0.08-0.15	0.10-0.16	0.08-0.15	0.08-0.15
Chromium	0.18-0.28 max	0.04 max	0.05 max	0.04 max	0.04 max

It has been suggested that replacing Cr by Zr results in low-quench-sensitivity (Mukhopadhyay et al., 1994), while the recrsytallization process can be desirably controlled (Ryum, 1969). The comparison of Zr and Cr contents of alloy AA7075 with high quench sensitivity alloys listed in Table 4 indicates a high level of Cr in AA7075, while the other alloys have minimized Cr, while containing a similar Zr content (0.08-0.15% by mass).

Figure 11 shows the stress-strain response obtained for both alloys that were quenched at 25°C/s, 40°C/s and 60°C/s and either tested immediately or allowed to naturally age for 6 days. For both alloys, these trends generally conform to the hardness measurements shown in Figure 9. The stress-strain curves of the naturally aged AA7xxx specimens were indistinguishable for the three quench rates considered, as were the curves for the three as-quenched conditions. This data demonstrates that the room temperature strengthening behavior of AA7xxx is not sensitive to the quench rates considered in Figure 11.

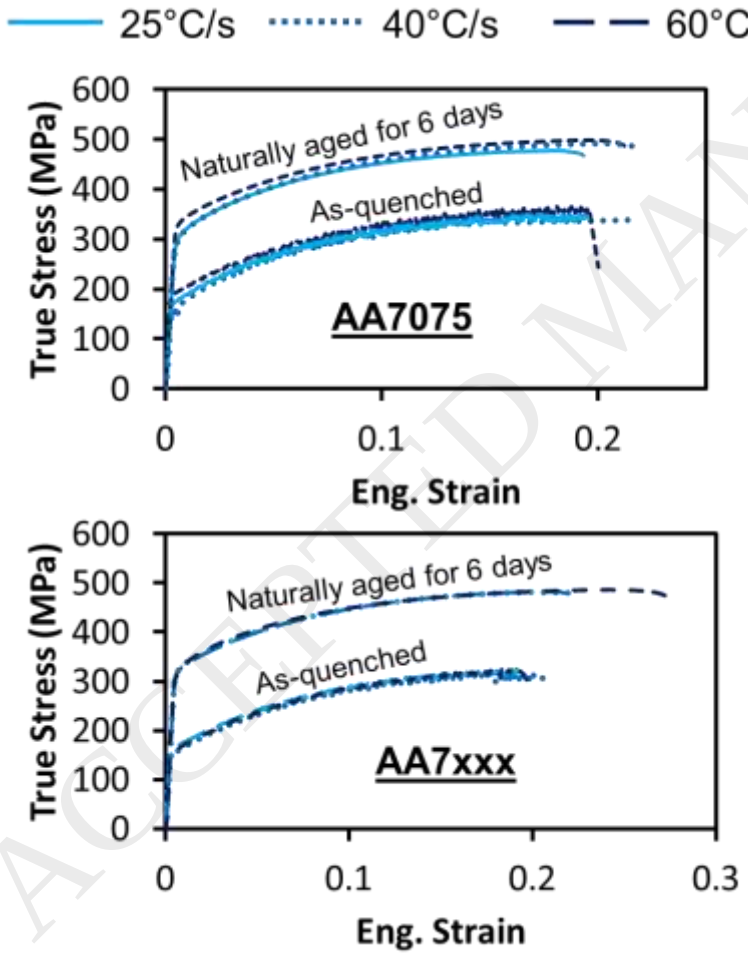

Figure 11. Stress-strain curves obtained from material quenched at different rates, immediately after quenching and six days after quenching while being stored at room temperature.

For AA7075, the as-quenched and naturally aged samples, did display a sensitivity to quench rate. The samples quenched at 25°C/s turned out to be the softest after six days of natural aging, and their strength increased successively for quench rates of 40°C/s and 60°C/s.

4.3.3. PLC Effect

It is important to mention that the serrations in the as-quenched stress-strain curves, particularly in the AA7xxx specimens, are evidence of the Portevin-Le Chatalier (PLC) effect that was also observed by Leacock et al. (2013) for AA7075. In their study on AA7475, Thevenet et al. (1999) attributed the serrations in the material stress-strain curve to the presence of magnesium atoms interacting with dislocations during deformation. Deschamps et al. (2012) found that deforming supersaturated AA7449 results in dynamic precipitation. Lang et al. (2011) made similar observations for AA7050.

To highlight the PLC effect, a FLIR SC8200 infrared camera was used to measure the temperature field during tensile deformation of an as-quenched AA7xxx tensile specimen. Figure 12 shows measured temperature contours of a die-quenched AA7xxx specimen tested in the rolling direction. Three temperature profiles along the length of the specimen were also plotted: one through the centre-line and two along the edges. The contours and the profiles show that there was a narrow band on the specimen that was approximately 1.2°C warmer than surrounding regions. The warmer location corresponded to an area of high effective strain, as shown in the contour plot of effective strain at the right in Figure 12 (strain contours were obtained through *in situ* DIC measurements).

During the experiment, multiple PLC bands were seen in the infrared video with more bands occurring at higher strain levels. Since the AA7xxx tensile specimen was in an SSSS state

dynamic precipitation may occur, as also suggested by (Deschamps et al., 2012; Pink, 1989). It is possible that local increases in strain rate associated with dynamic precipitation could lead to a local increase in release of heat.

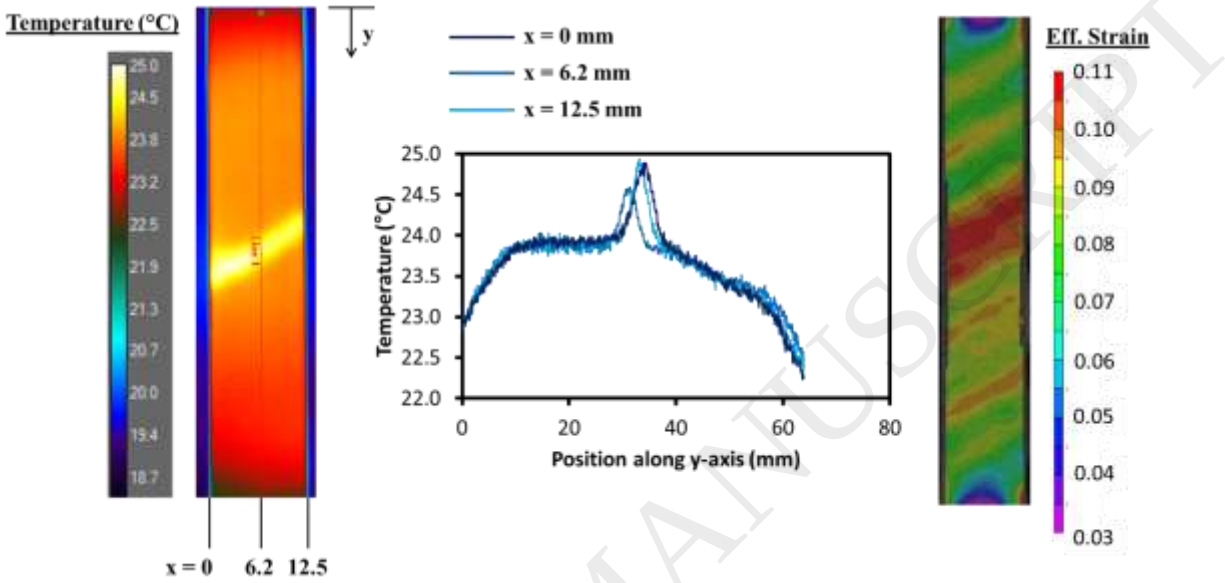

Figure 12. Temperature profile and strain bands in an as-quenched AA7xxx tensile specimen at an elongation of 5 mm. Multiple local temperature fluctuations were observed during deformation.

4.4. Artificial Aging Parameters

The motivation for the artificial aging process design in this work is to achieve mechanical properties that are as close as possible to the peak strength T6, or the overaged T76 conditions while leveraging the secondary paint bake treatment to contribute to the precipitation hardening and reduce the aging heat treatment duration relative to that required for a conventional T6/T76 aging treatment (121°C for 24h for AA7075-T6 (ASM International, 1990) and 120°C for 5h then 163°C for 15h for AA7085-T76 (U.S. Government Printing Office, 1991)).

4.4.1. Experimental Setup – AA7075

A two-step aging process was considered in which the first stage utilized the conventional aging temperature of 121°C while the second stage comprised a PBC of 177°C for 30 minutes. Samples were first solutionized at 470°C for 8 minutes, followed by a 6s transfer, and then a 34°C/s quench rate. The objective of these experiments was to determine the duration of the first stage at 121°C such that the two-stage aging resulted in mechanical properties close to those in the T6 condition. Conceptually, this two-stage treatment can be considered an "interrupted T6 treatment, followed by a paint bake cycle"; hence, the T6IPB designation adopted herein. All artificial aging was performed within 20 minutes of quenching.

To this end, hardness measurements were conducted on AA7075 samples that were heat treated at 121°C for the following times: 30 min, 1h, 2h, 4h, 8h, 12h, 16h, 24h, 48h and 72h. All of the samples were subject to a PBC after their initial heat treatment at 121°C. To further examine the aging response using this two-stage aging treatment, tensile tests were performed on samples aged at 121°C for 4h, 8h and 12h and then paint baked. All tensile tests were conducted in the rolling direction of the sheet.

In addition to the hardness and tensile measurements, differential scanning calorimetry (DSC) was performed on selected tempers of AA7075. A Setaram C80 calorimeter was used with a heating rate of 1°C/s, starting from 25°C and heating up to 300°C. The DSC experiments were run in an air atmosphere where the reference vessel was empty. The DSC samples were subjected to the same heat treatment conditions as those that were used for tensile samples. In addition to these samples, a baseline run was conducted on pure aluminum. The DSC curves presented in this paper were obtained by subtracting the DSC trace obtained for pure aluminum from the DSC trace obtained for the heat treated sample. Two repeats were conducted per

condition on samples weighing 925 ± 10 mg. The two repeats were found to be very similar, so only one test per condition is presented.

4.4.2. Results – AA7075

The hardness measurements are shown in Figure 13, from which it can be seen that hardness increases for first stage durations of up to 8h. Beyond 8h, the hardness drops due to overaging. Interestingly, the hardness corresponding to the aging cycle incorporating an 8h duration for the first stage corresponds to that of the conventional T6 peak aged condition. Figure 14 shows the stress-strain curves, along with data for the T6 temper (aged for 24h at 121°C after being solutionized and quenched) shown in Figure 4. The samples utilizing a first stage aging duration of 8h exhibited a stress-strain response in close accord with that of the as-received T6 temper. Accordingly, the temper condition corresponding two-stage aging treatment is hereafter designated T6IPB (I for interrupted, PB for paint bake).

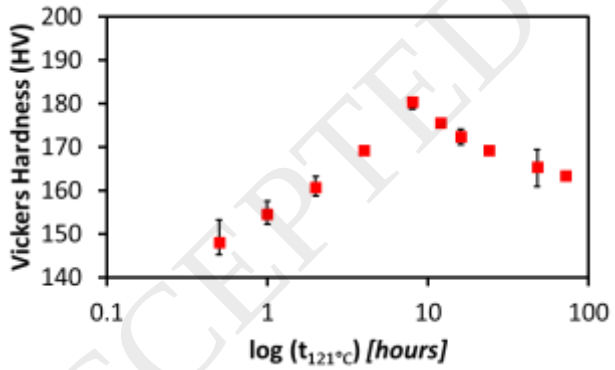

Figure 13. Hardness measurements for AA7075 samples subject to a two-step heat treatment: starting with 121°C at various times (shown on the plot), followed by a PBC.

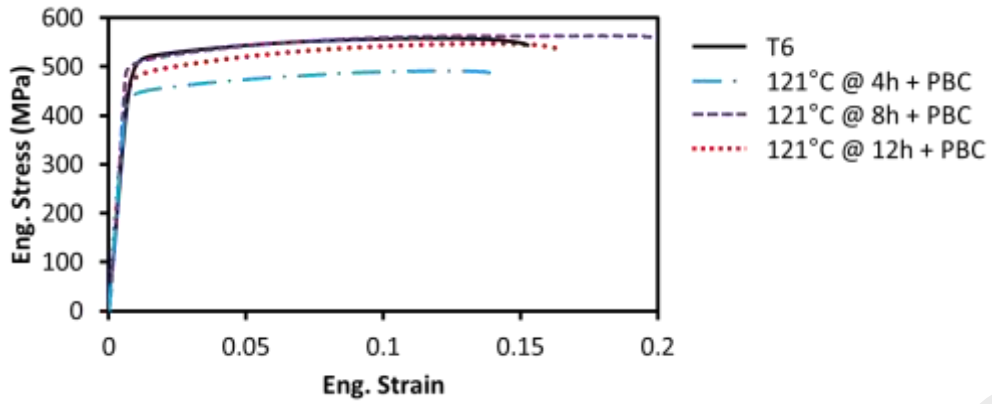

Figure 14. Measured stress-strain curves of AA7075 subjected to heat treatment at 121°C for 4h, 8h and 12h, followed by a PBC. The stress-strain curve for a conventional T6 heat treatment is also shown for reference.

The results of the DSC experiments on the AA7075 alloy are shown in Figure 15. The W-temper exhibited four main peaks, which are marked I, II, III and IV in Figure 15. Peak I corresponds to the formation of GP zones (Deschamps and Bréchet, 1998). It is no surprise that peak I disappears entirely for the other four tempers in Figure 15, since the GP zones from the W-temper are expected to be formed after the heat treatments that were applied prior to the DSC run. Peaks II and III likely correspond to the formation of η' precipitates and the transformation of η' into η precipitates, respectively (Deschamps and Bréchet, 1998). Peak IV was likely linked to the formation of the T phase (Hadjadj et al., 2008). None of these peaks were present in the 12h at 121°C + PBC temper, which is considered a slightly overaged temper based on Figure 14. These peaks were also not present in the T6 and T6IPB tempers, which are peak-aged tempers. Instead, both tempers exhibit two, small endothermic peaks, which can be linked to the dissolution of the η' precipitates (Kumar and Ross, 2016). The 4h at 121°C + PBC temper, being an under-aged temper, did contain peaks II, III and IV, although peak II is very small in magnitude compared to the W-temper.

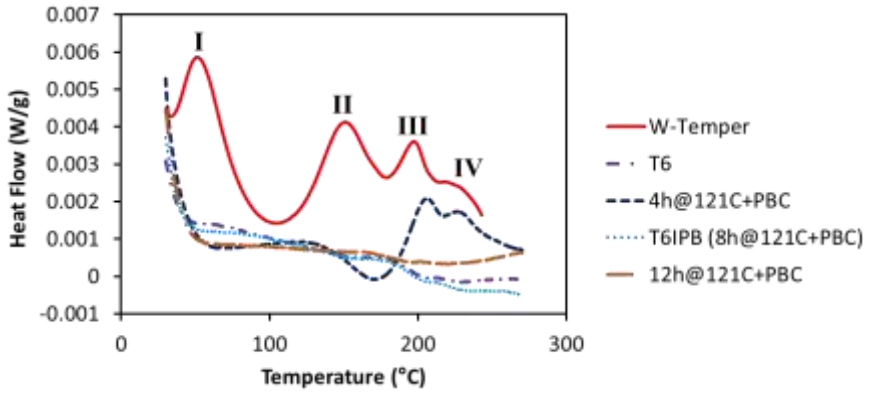

Figure 15. DSC curves for selected tempers on AA7075. The upwards direction indicates exothermic flow.

4.4.3. Experimental Setup – AA7xxx

For AA7xxx, samples were first solutionized at 470°C for 8 minutes, followed by a 6s transfer, and then a 34°C/s quench rate. Afterwards, the samples were artificially aged at several aging temperatures: 100°C, 120°C, 135°C, 150°C and 163°C. The temperatures 120°C and 163°C were chosen because they correspond to the two temperatures used in a T76 treatment. The remaining temperatures were selected as intermediate conditions. A PBC followed all of the artificial aging treatments. Hardness measurements were conducted on samples subjected to each of these processing routes. In addition, hardness tests were performed on samples aged at 120°C for various times but without a paint bake cycle; this set of experiments served to determine the aging time to reach a T6 temper. Tensile tests were also conducted at certain temperatures identified as critical from the hardness measurements: 100°C for 4h + PBC, 120°C for 4h + PBC, 135°C for 4h + PBC. All artificial aging was performed within 20 minutes of quenching.

4.4.4. Results – AA7xxx

The results of the hardness tests are shown in Figure 16. The hardness data in Figure 16a shows that AA7xxx attains a peak aged condition when aged at 120°C for 20 hours (*i.e.*, a T6 condition). This condition, with a peak hardness of 176 HV, was taken as an estimate of the T6

hardness, which is 5% higher than the hardness in the T76 as-received condition (167 HV). Figure 16b shows the measured hardness resulting from the two-stage aging processes in which the paint bake cycle serves as the second stage. For such a two-stage treatment, AA7xxx achieves hardness levels that are very close to the T6 condition with a first stage heat treatment of only 3 hours at 120°C followed by a paint bake. This heat treatment (3h at 120°C + PBC) was designated in this work as a T6IPB temper for AA7xxx.

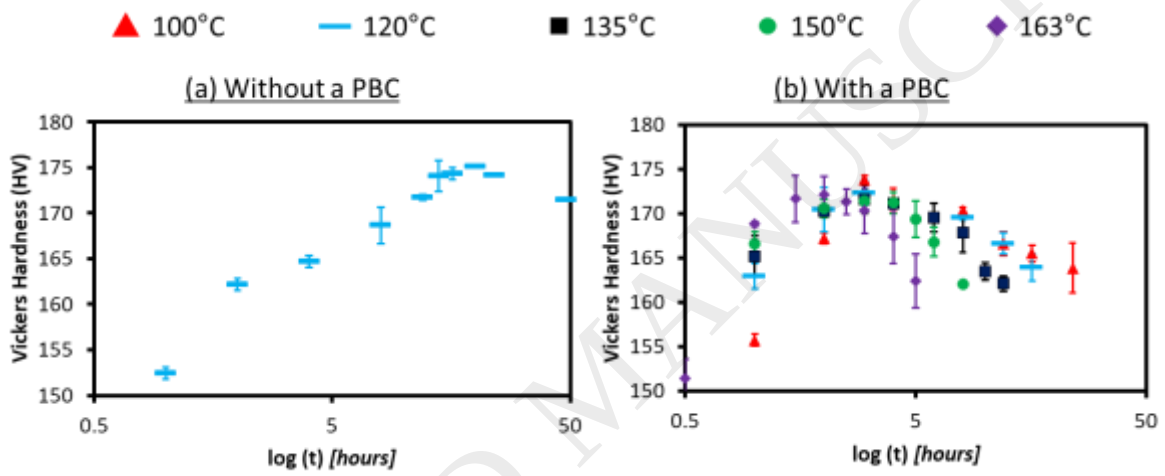

Figure 16. Hardness measurements for AA7xxx samples aged at various temperatures for various times (a) without a PBC and (b) with a PBC.

The tensile test results shown in Figure 17a confirm that the custom T6IPB temper exhibits properties similar to T6. The close-up of the stress-strain curves in Figure 17c shows that the T6IPB stress level is within 10 MPa of the T6 response and displays similar hardening response. It is recognized that a slightly higher hardness (174 HV) was attained for a first stage aging treatment of 100°C for 3 hours followed by PBC. The 120°C initial aging temperature was adopted for the T6IPB first stage aging treatment since it utilized the 120°C temperature of the standard T6 aging treatment.

As for achieving properties similar to a T76 temper, Figure 16 shows that several aging routes incorporating a PBC can achieve this hardness level. To select a "T76IPB" temper for the purposes of this study, tensile tests were conducted for various temperatures, all of which yielded a hardness value similar to that of AA7xxx-T76 (~168 HV) and corresponded to over-aged conditions from Figure 14. The heat treatment whose stress-strain curve mostly closely matched the AA7xxx-T76 response was 100°C for 4h + PBC. Therefore, this treatment was selected as the T76IPB temper for AA7xxx.

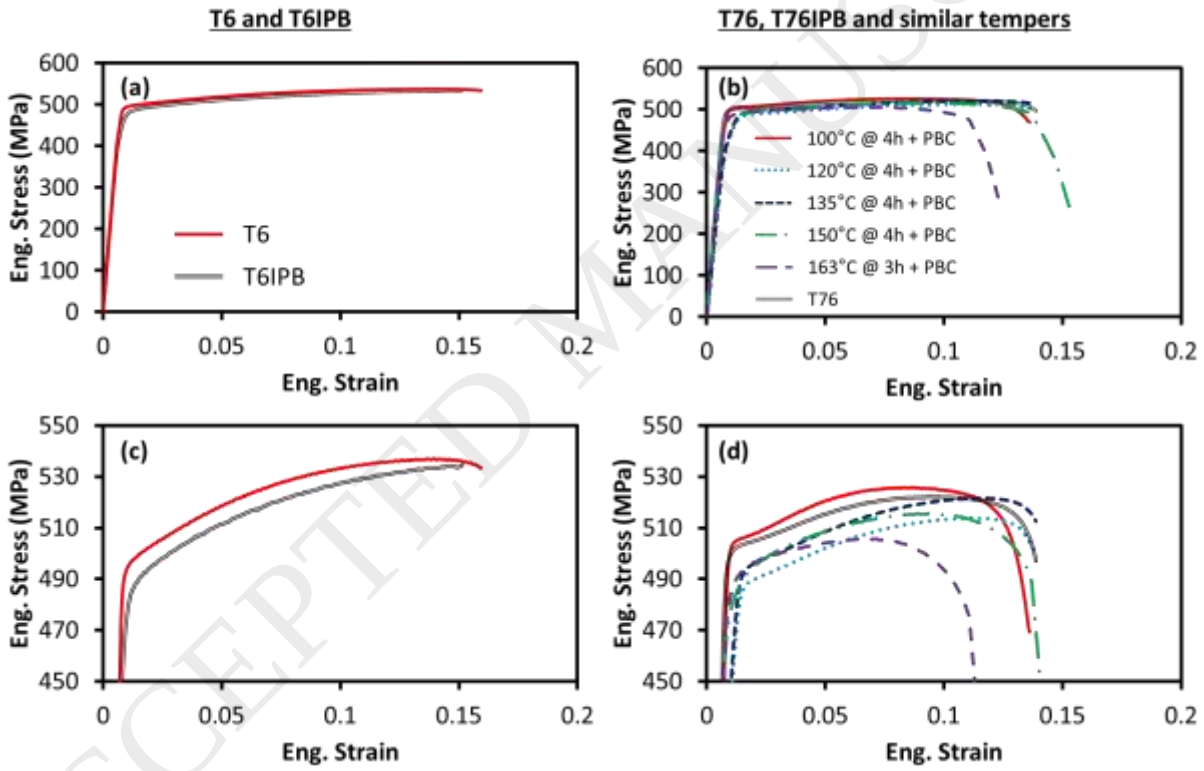

Figure 17. Stress-strain curves obtained from tensile tests for (a), (c) AA7xxx-T6 and -T6IPB, and (b), (d) several aging routes incorporating a PBC that yield in a hardness value similar to AA7xxx-T76. For reference, the T76 properties from Figure 4 are also shown. Note that (c) and (d) are magnified views of (a) and (b), respectively.

4.5. Summary of Processing Parameters

Based on the results presented in the previous sections of this paper, DQ processing routes were selected for AA7075 and AA7xxx. Parameters were selected to limit total aging time and to

achieve high strength in the as-processed materials for a thermal history that includes exposure to the paint bake cycle. The selected parameters are shown in Table 5.

Table 5. Selected DQ process parameters

Parameter	AA7075-T6IPB	AA7xxx-T6IPB	AA7xxx-T76IPB
Solutionizing Time	8 min	8 min	8 min
Solutionizing Temperature	470°C	470°C	470°C
Minimum Quench Rate	56°C/s	27°C/s	27°C/s
First Stage Artificial Aging Time	8h	3h	4h
First Stage Artificial Aging Temperature	121°C	120°C	100°C
Paint Bake Cycle	177°C for 30 min	177°C for 30 min	177°C for 30 min

5. Discussion

The experiments conducted in this work show that the developmental AA7xxx alloy is an excellent candidate for the DQ process. It exhibits low sensitivity to quench rate for the rates considered in this study. AA7075, however, does exhibit sensitivity to quench rate for the range considered in this study, as highlighted by the variation in stress-strain curves in Figure 11. A minimum quench rate of 40°C/s is required for this alloy for maximum age hardenability, assuming no significant deformation occurs during quenching. A higher quench rate may be needed if deformation is applied. The higher quench rate would cool the part quicker and, therefore, the material would be less prone to heterogenous solute precipitation (Poole and Shercliff, 1996) and excess vacancy annihilation during quenching (Fabian and Wolter, 1991).

In addition to being advantageous in quench rates, AA7xxx is also more appealing than AA7075 in its transfer time requirement. AA7075 requires a shorter minimum transfer time between the furnace and tooling than can be tolerated by AA7xxx. AA7xxx was found to tolerate a transfer

time of up to 15s, whereas AA7075 lost some elongation at this transfer time. In fact, a transfer time of over 6s will likely cause issues in age hardenability in this alloy since it reaches its critical temperature of 415°C in this time. After 6s, solute precipitation will begin, which will affect the age hardenability of AA7075. AA7xxx does not reach its critical temperature till after 15s of air cooling, and therefore, has a higher tolerance window in transfer time. Once in the press being die quenched, the cooling rate of AA7xxx increases, which will lower its critical temperature (Yang et al., 2016), thereby enabling a successful entry into the supersaturated phase. Both alloys were found to require a heating time of 8 minutes in the convection furnace for the current 2 mm thickness. The 8 minute heat-up time corresponded to a 90s soak time at the solutionizing temperature of 470°C.

The work presented herein also demonstrates an artificial aging route that can be used in conjunction with the paint bake cycle to achieve T6 or T76 mechanical properties for the heat treated material. By incorporating the paint bake cycle into the process design of the component, the total treatment or aging time is reduced significantly for both AA7075 and AA7xxx. For AA7075, the aging time reduced from 24h for a standard T6 treatment to 8.5h for a T6IPB treatment, which includes the PBC. For AA7xxx, the treatment time reduced from 16h for a T6 treatment to 3.5h for a T6IPB treatment. Furthermore, the treatment time reduced from 20h for T76 to 4.5h for T76IPB.

Future work includes corrosion testing of these alloys in the alternate temper conditions to assess whether the IPB aging treatments affect corrosion resistance relative to the T6 or T76 conditions. The assessment of the high strain rate behaviour of these alloys, in terms of both constitutive and fracture response to elevated strain rate, is also important in order to support their application in crash safety structures.

6. Conclusions

The work presented in this paper shows the required DQ processing parameters in order reach a SSSS for the AA7075 and AA7xxx alloys. AA7xxx was found to exhibit very favourable properties for the DQ process, including its low sensitivity to quench rate and transfer time as well as its fast age hardenability when subjected to a PBC. AA7075 was found to be more sensitive than AA7xxx to quench rate and transfer time. The processing routes identified for both alloys (T6IPB and T76IPB) reduce the total aging time of the two alloys considerably, while incorporating a PBC. Future work should evaluate the corrosion performance of these alloys in the IPB tempers, as well as their mechanical behaviour when formed into structural components.

Acknowledgments

The authors would like to thank Honda R&D Americas Inc., Arconic Ground Transportation Group, Promatek Research Centre, the Natural Sciences and Engineering Research Council (NSERC), the Canada Foundation for Innovation, and the Canada Research Chairs Secretariat for supporting this research.

References

ASM International, 1990. Metals Handbook. ASM International.

Atkinson, H.V., Burke, K., Vaneetveld, G., 2008. Recrystallisation in the semi-solid state in 7075 aluminium alloy. Mater. Sci. Eng. A 490, 266–276. doi:10.1016/j.msea.2008.01.057

Caron, E.J.F.R., Daun, K.J., Wells, M. a., 2014. Experimental heat transfer coefficient measurements during hot forming die quenching of boron steel at high temperatures. Int. J. Heat Mass Transf. 71, 396–404. doi:10.1016/j.ijheatmasstransfer.2013.12.039

Chen, S., Chen, K., Peng, G., Jia, L., Dong, P., 2012. Effect of heat treatment on hot deformation behavior and microstructure evolution of 7085 aluminum alloy. Mater. Des. 25, 93–98.

Clark, R., Coughran, B., Traina, I., Hernandez, A., Scheck, T., Etuk, C., Peters, J., Lee, E.W.,

Ogren, J., Es-Said, O.S., 2005. On the correlation of mechanical and physical properties of 7075-T6 Al alloy. Eng. Fail. Anal. 12, 520–526. doi:10.1016/j.engfailanal.2004.09.005

Conserva, M., Di Russo, E., Caloni, O., 1971. Comparison of the influence of chromium and zirconium on the quench sensitivity of Al-Zn-Mg-Cu alloys. Metall. Trans. 2, 1227–1232. doi:10.1007/BF02664256

Correlated Solutions, 2013. Vic 3D - 7.

Deschamps, A., Fribourg, G., Brechet, Y., Chemin, J.L., Hutchinson, C.R., 2012. In situ evaluation of dynamic precipitation during plastic straining of an Al-Zn-Mg-Cu alloy. Acta Mater. 60, 1905–1916. doi:10.1016/j.actamat.2012.01.002

Deschamps, a., Bréchet, Y., 1998. Influence of quench and heating rates on the ageing response of an Al–Zn–Mg–(Zr) alloy. Mater. Sci. Eng. A 251, 200–207. doi:10.1016/S0921-5093(98)00615-7

Erdoğan, M., Erçetin, A., Güneş, İ., 2014. Investigation of Mechanical Properties of Natural Aged Aa 7075 Aluminum Alloy 15–17.

Fabian, H.G., Wolter, R., 1991. Determination of the Effective Vacancy Concentrations and the Vacancy Losses after the Quench of Al–Zn–Mg Alloys. Cryst. Res. Technol. 26, 93–102. doi:10.1002/crat.2170260117

Hadjadj, L., Amira, R., Hamana, D., Mosbah, A., 2008. Characterization of precipitation and phase transformations in Al-Zn-Mg alloy by the differential dilatometry. J. Alloys Compd. 462, 279–283. doi:10.1016/j.jallcom.2007.08.016

Jabra, J., Romios, M., Lai, J., Lee, E., Setiawan, M., Lee, E.W., Witters, J., Abourialy, N., Ogren, J.R., Clark, R., Oppenheim, T., Frazier, W.E., Es-Said, O.S., 2006. The Effect of Thermal Exposure on the Mechanical Properties of 2099-T6 Die Forgings, 2099-T83 Extrusions, 7075-T7651 Plate, 7085-T7452 Die Forgings, 7085-T7651 Plate, and 2397-T87 Plate Aluminum Alloys. J. Mater. Eng. Perform. 15, 601–607. doi:10.1361/105994906X136142

Kumar, M., Ross, N.G., 2016. Influence of temper on the performance of a high-strength Al-Zn-Mg alloy sheet in the warm forming processing chain. J. Mater. Process. Technol. 231, 189–198. doi:10.1016/j.jmatprotec.2015.12.026

Lang, Y., Cai, Y., Cui, H., Zhang, J., 2011. Effect of strain-induced precipitation on the low angle grain boundary in AA7050 aluminum alloy. Mater. Des. 32, 4241–4246. doi:10.1016/j.matdes.2011.04.025

Leacock, A.G., Howe, C., Brown, D., Lademo, O.G., Deering, A., 2013. Evolution of mechanical properties in a 7075 Al-alloy subject to natural ageing. Mater. Des. 49, 160–167. doi:10.1016/j.matdes.2013.02.023

Liu, S. dan, Zhang, X. ming, Chen, M. an, You, J. hai, Zhang, X. yan, 2007. Effect of Zr content on quench sensitivity of AlZnMgCu alloys. Trans. Nonferrous Met. Soc. China (English Ed. 17, 787–792. doi:10.1016/S1003-6326(07)60175-7

Liu, S., Zhong, Q., Zhang, Y., Liu, W., Zhang, X., Deng, Y., 2010. Investigation of quench sensitivity of high strength Al-Zn-Mg-Cu alloys by time-temperature-properties diagrams.

Mater. Des. 31, 3116–3120. doi:10.1016/j.matdes.2009.12.038

Mohamed, M.S., Foster, A.D., Lin, J., Balint, D.S., Dean, T. a., 2012. Investigation of deformation and failure features in hot stamping of AA6082: Experimentation and modelling. Int. J. Mach. Tools Manuf. 53, 27–38. doi:10.1016/j.ijmachtools.2011.07.005

Mukhopadhyay, A.K., Yang, Q.B., Singh, S.R., 1994. The influence of zirconium on the early stages of aging of a ternary AlZnMg alloy. Acta Metall. Mater. 42, 3083–3091. doi:10.1016/0956-7151(94)90406-5

Pink, E., 1989. The effect of precipitates on characteristics of serrated flow in AlZn5Mg1. Acta Metall. 37, 1773–1781. doi:10.1016/0001-6160(89)90062-X

Poole, W.J., Shercliff, H.R., 1996. The effect of deformation prior to artificial ageing on the ageing characteristics of a 7475 aluminum alloy. Mater. Sci. Forum 217–222, 1287–1292. doi:10.4028/www.scientific.net/MSF.217-222.1287

Rajamuthamilselvan, M., Ramanathan, S., 2011. Hot deformation behaviour of 7075 alloy. J. Alloys Compd. 509, 948–952. doi:10.1016/j.jallcom.2010.09.139

Ryum, N., 1969. Precipitation and recrystallization in an A1-0.5 WT.% Zr-alloy. Acta Metall. 17, 269–278. doi:10.1016/0001-6160(69)90067-4

Sevim, I., Sahin, S., Cuz, H., Cevik, E., Hayat, F., Karali, M., 2014. EFFECT OF AGING TREATMENT ON SURFACE ROUGHNESS, MECHANICAL PROPERTIES, AND FRACTURE BEHAVIOR OF 6XXX AND 7XXX ALUMINUM ALLOYS. Strength Mater. 46, 190–197.

Standard Test Methods for Tension Testing of Metallic Materials, 2015.

Starink, M.J., Milkereit, B., Zhang, Y., Rometsch, P.A., 2015. Predicting the quench sensitivity of Al-Zn-Mg-Cu alloys: A model for linear cooling and strengthening. Mater. Des. 88, 958–971. doi:10.1016/j.matdes.2015.09.058

The Aluminum Assosciation, 2009. International Alloy Designations and Chemical Composition Limits for Wrought Aluminum and Wrought Aluminum Alloys.

Thevenet, D., Mliha-Touati, M., A, Z., 1999. The effect of precipitation on the Portevin-Le Chatelier effect in an Al–Zn–Mg–Cu alloy. Mater. Sci. Eng. A 266, 175–182. doi:10.1016/S0921-5093(99)00029-5

U.S. Government Printing Office, 1991. Heat Treatment of Aluminum Alloys. MI L -H- 6088G.

Viana, F., Pinto, a. M.P., Santos, H.M.C., Lopes, a. B., 1999. Retrogression and re-ageing of 7075 aluminium alloy: microstructural characterization. J. Mater. Process. Technol. 92–93, 54–59. doi:10.1016/S0924-0136(99)00219-8

Wang, H., Luo, Y., Friedman, P., Chen, M., Gao, L., 2012. Warm forming behavior of high strength aluminum alloy AA7075. Trans. Nonferrous Met. Soc. China 22, 1–7. doi:10.1016/S1003-6326(11)61131-X

Xie, F., Yan, X., Ding, L., Zhang, F., Chen, S., Chu, M.G., Chang, Y.A., 2003. A study of microstructure and microsegregation of aluminum 7050 alloy. Mater. Sci. Eng. A 355, 144–153. doi:10.1016/S0921-5093(03)00056-X

Yang, B., Milkereit, B., Zhang, Y., Rometsch, P.A., Kessler, O., Schick, C., 2016. Continuous cooling precipitation diagram of aluminium alloy AA7150 based on a new fast scanning calorimetry and interrupted quenching method. Mater. Charact. 120, 30–37. doi:10.1016/j.matchar.2016.08.016

Zhang, H., Nagaumi, H., Zuo, Y., Cui, J., 2007. Coupled modeling of electromagnetic field, fluid flow, heat transfer and solidification during low frequency electromagnetic casting of 7XXX aluminum alloys: Part 1: Development of a mathematical model and comparison with experimental results. Mater. Sci. Eng. A 448, 189–203. doi:10.1016/j.msea.2006.10.062

Zhang, Y., Milkereit, B., Kessler, O., Schick, C., Rometsch, P.A., 2014. Development of continuous cooling precipitation diagrams for aluminium alloys AA7150 and AA7020. J. Alloys Compd. 584, 581–589. doi:10.1016/j.jallcom.2013.09.014

Zhang, Y., Weyland, M., Milkereit, B., Reich, M., Rometsch, P.A., 2016. Precipitation of a new platelet phase during the quenching of an Al-Zn-Mg-Cu alloy. Sci. Rep. 6, 23109. doi:10.1038/srep23109